

Direct observation of pinned/biased moments in magnetic superlattices

P. Padhan and W. Prellier*

*Laboratoire CRISMAT, CNRS UMR 6508, ENSICAEN,
6 Bd du Maréchal Juin, F-14050 Caen Cedex, FRANCE.*

(November 9, 2018)

Abstract

We report the *pinned/biased moment* in the superlattices consisting of ferromagnetic (FM) SrRuO₃ and antiferromagnetic (AFM) SrMnO₃. This superlattice system shows anisotropy and oriented pinning/biasing in the field-cooled (FC) hysteresis loop. The in-plane cooling-field provides antiferromagnetic orientations while out-of-plane cooling-field provides ferromagnetic orientations to the pinned/biased moments. The spacer layer thickness, strength and orientation of magnetic field, cooling field, and driving current influence the pinning strength. We propose that the magnetic structure is a repetition of *AFM/Pin/FM(Free)/Pin* unit below a critical field to explain its magnetic and transport properties. The transport behavior is discussed using the spin-dependent conduction.

*prellier@ensicaen.fr

A biased magnetic field has been observed on cooling the FM-AFM system below the Curie temperature (T_C) of the *FM* through the Neel temperature (T_N) of the *AFM* in presence of a magnetic field¹⁻⁵. It is believed that the biased field is responsible for the shift of the hysteresis loop along the field axis which has been observed in a wide variety of *FM - AFM* systems, many of which do not exhibit a simple spin structure at the interface to the *FM -AFM* layers or materials. In general, a biased field is established through field-cooling in the film plane where the magnetic easy axis of soft ferromagnetic materials normally lies in plane. A shift in hysteresis loop along the magnetization axis in addition to the shift along the field axis is also observed⁶. The authors have explained the shift in hysteresis loop along the magnetization axis by the pinned uncompensated spin at the interfaces. Recently Maat *et al.*⁷ have shown that exchange bias can also be observed for the magnetization perpendicular to the film plane in *Co/Pt* multilayers biased by *CoO*. They investigated the biasing in various directions and found substantially more within the sample plane, which they related to the anisotropy of the single-*q* spin structure of the *CoO*. Several theoretical models have been proposed to explain the origin of the biased field. Indeed, most of the theoretical models assume a single domain state of the ferromagnetic layer and focus on the domain structure of the *AFM* layer for different types of interfaces. However, despite the enormous research done in this field, this effect is poorly understood.

Here, we report the direct observation of pinned/biased moments of the *SrRuO₃* (*SRO*) layers by the *SrMnO₃* (*SMO*) layers in the *SRO/SMO* superlattices grown on (001)-*SrTiO₃* (*STO*) substrates. To the best of our knowledge, this observation has not been reported so far. The presence of pinned/biased effect can be realized in the magnetic hysteresis loop with field range below certain critical magnetic field (H_P). Various factors such as the *SMO* layer thickness, strength and orientation of the external magnetic field and cooling field influenced the strength of the pinned/biased moments of *SRO*, thus providing a way to control it. Consequently, this presents the tantalizing possibility of controlling the pinning of a *FM* layer by the *AFM* layer in an oxide multilayer, which is a necessary step towards a better understanding and improvement of modern magnetic devices.

The fabrication with optimized growth conditions and structural characterizations of the superlattices have been reported elsewhere⁸. The superlattice structures were synthesized by repeating 15 times the bilayer comprising of 20-(*unit cell, u.c.*) *SRO* and n -(*u.c.*) *SMO*, with n taking integer values from 1 to 20. In all superlattices, *SRO* is the bottom layer and the modulated structure was covered with 20 *u.c.* *SRO* to keep the structure of the top *SMO* layer stable. The samples were characterized by resistivity (ρ) and magnetization (M) measurements, in addition to x-ray diffraction and transmission electron microscopy. Transport and magnetization measurements were performed at 10 *K* with magnetic field along the [100] and [001] directions of *STO*. The samples were cooled to a desired temperature (T) from room temperature in the absence of electric and magnetic field to perform zero-field-cooled (*ZFC*) measurements. The field-cooled (*FC*) measurements were always performed with the same orientation of cooling field.

SrRuO₃ is known as a metallic *FM*, with a Curie temperature (T_C) \sim 160 *K* in its bulk form⁹. Similar transport and magnetic behaviors are observed in (80 *nm*)*SRO/STO* with easy axis along [001] direction of *STO*, consistent with Ref.10. The saturation field (H_S), coercive field (H_C) and saturation magnetization (M_S) along the easy axis of this film are 0.4 *tesla*, 0.17 *tesla* and 1.46 μ_B/Ru , respectively. Its *ZFC* and *FC* magnetic hysteresis loop ($M - H$) remain the same at 10 *K* under 0.1 *tesla* cooling field (H_{FC}). The current-in-plane magnetoresistance (*MR*) of this sample with magnetic field along [100] and [001] directions of the *STO* is negative although it is hysteretic and higher when $H \perp I$. In contrast, *SrMnO₃* is an *AFM* with a Neel temperature close to 260 *K*¹¹ and crystallizes in a cubic structure when sandwiched between perovskite layers inside a superlattice⁸.

Fig. 1 shows the zero-field-cooled (*ZFC*) magnetization at 10 *K* at various magnetic fields oriented along the in-plane and out-of-plane directions of the substrate for the sample with 3 *u.c.* thick *SMO* layer. The easy axis of *SRO* remains same in the superlattices. The in-plane magnetization of the superlattice gradually increases as the magnetic field increases and becomes larger than the calculated value (1.6 μ_B/Ru), based on the only contribution from *SRO* layer. This larger value of the in-plane magnetization indicates that the *SMO* layer

contribute to the net magnetization of the superlattice at higher magnetic field. However, the out-of-plane hysteresis loop shows a clear M_S and H_S with enhanced H_C . In order to understand the strong anisotropic nature of the ferromagnetic layer in the superlattice and their magnetotransport behavior below H_C , we have measured the minor hysteresis loops of this superlattice in the field range between the saturation field of SRO and the out-of-plane H_C of the superlattice with $n = 3$. The minor ZFC hysteresis loops in the field range of ± 1 tesla are symmetric with respect to the origin (Fig. 2a and 2b) for magnetic field along the [100] and [001] directions of *STO*. The gradual increase in magnetization with the increase in magnetic field even above the H_S (0.4 tesla) of *SRO* indicates that the spin-orbit coupling is modified in *SRO* layer and that the MnO_6 octahedra at the interface influences the magnetic state of the RuO_6 octahedra^{12,13}. The H_C of *SRO* layer (0.02 tesla along [100] and 0.17 tesla along [001]) is reduced in the superlattices (0.001 tesla and 0.0027 tesla respectively). The magnetization of *SRO* layer ($1.46 \mu_B/Ru$) is decreased to $\approx 0.6 \mu_B/Ru$ in the superlattices. This large suppression of the *FM* state of the SRO layer in the superlattice suggests that it is strongly influenced by the *G*-type *AFM* state of the *SMO* layer¹¹. In the case of *G*-type spin ordering, the (00*l*) planes show the staggered pattern of spin arrangement, which is the source of spin frustration at the compensated *SRO* – *SMO* interfaces as well as the spin canting in the *SRO* layer in the vicinity of the interfaces¹⁴. Thus, due to the presence of *SMO* layer, the spin canting/frustration in the *SRO* layer is reducing the effective *FM* layer thickness of the SRO layer in the *SRO/SMO* superlattice. In others words, the effective ferromagnetic *SRO* layer thickness is decreasing by the presence of a canted/frustrated spin in the SRO layer close to the interface, which will be detailed hereafter (Fig.5b).

In general, the magnetic interactions across the interface between the *FM* and *AFM* are known as exchange coupling (*EC*), with phenomenological features such as an enhancement and an unidirectional anisotropy of H_C ¹⁻⁵. To study the exchange coupling at the *FM* – *AFM* interfaces, we have measured the *FC* hysteresis loop of this sample. The *FC* hysteresis loop of the superlattice with $n = 3$ for in-plane and out-of-plane orientations of the

magnetic field are shown in Fig. 2a and 2b respectively. It shows several interesting features. First, the center of in-plane as well as out-of-plane FC hysteresis loop is shifted along the magnetization axis. Second, the FC hysteresis loops show a negligibly small change in the values of H_C compared to the ZFC hysteresis loop. Third, the values of the in-plane magnetization in the FC hysteresis loop is lower (Fig. 2a) while the out-of-plane magnetization in the FC hysteresis loop is higher (Fig. 2b) than its corresponding magnetization in the ZFC hysteresis loop. These features indicate that the spin configuration that was realized in the ZFC state is modified in presence of cooling magnetic field. From the observed ZFC and FC hysteresis loop one can conclude that the canted/frustrated spins are aligned anti-ferromagnetically in the presence of in-plane cooling-field and are aligned ferromagnetically for out-of-plane cooling-field. So we define the oriented interfacial canted/frustrated spins as the pinned/biased moments at the interfaces. The in-plane pinned/biased moment can be defined as $M_P^{\parallel} = M_S(0) - M_S(H_{FC})$. Taking into account the weak diamagnetic response of the substrate, the M_S has been extracted by extrapolating the linear part of the $(M - H)$ curve to $H = 0$. The value of M_P^{\parallel} when H is antiparallel to H_{FC} is larger by $\approx 0.302 \times 10^{-4} \text{ emu}$ (a factor of 0.3) compared to the value of M_P^{\parallel} when H parallel to H_{FC} . This indicates the presence of moments at the interfaces which do not flip 180° with the flipping of the magnetic field. So the canted/frustrated layer, partially close to the $SRO - SMO$ interface, is pinned/biased along the direction of the cooling magnetic field. In other words, *this is a signature of uniaxial pinning/biasing of moments at the interfaces*. The value of M_P^{\parallel} changes significantly at cooling fields below $\pm 0.03 \text{ tesla}$ and remains constant for higher values of H_{FC} . Similarly, the out-of-plane pinned/biased moment M_P^\perp can be defined by analogy to the bias field as $M_P^\perp = \frac{M_R^+ + M_R^-}{2}$, where M_R^+ and M_R^- are field-increasing and field-decreasing remanent magnetization respectively. The same sign of the field for increasing and decreasing M_R (Fig. 2b) indicates the *uniaxial pinning/biasing of moments*. The value of M_P^\perp increases with H_{FC} and changes negligibly when $H_{FC} > 0.1 \text{ tesla}$. M_P^\perp also depends on the magnetic field that is applied and becomes zero when a magnetic field larger than 1.5 tesla is applied. We have also measured the M_P^\perp for various superlattices and the results are

given in Fig. 3. It decreases as the *SMO* layer thickness increases above 1 *u.c.*, and remains the same for $n > 7$. Since M_P^\perp varies with *SMO* layer thickness, this indicates that the *EC* at the interfaces is a combination of the exchange coupling (J_{exch}) between *SRO* layer and *SMO* layer and the interlayer exchange coupling (J_{int}) between the *SRO* layers. Note that for *SRO/SMO* superlattice, the Neel temperature of *SMO* layer is higher than the Curie temperature of *SRO* layer. Since the exchange coupling also depends on the thermal energy, the physical processes responsible for the effective exchange coupling ($J_{eff} \sim J_{exch} + J_{int}$) is expected to be different from the AFM/FM system where $T_C > T_N$.

From the ZFC and FC magnetization measurements of the *SRO/SMO* superlattices, we have observed a strong anisotropy and pinned/biased moments. To understand the effects of these magnetic behavior we have also studied their electronic transport in presence of magnetic field below H_P . The ZFC and FC current-in-plane magnetoresistance for various magnetic fields (*MR - H*) in the range of magnetic field (± 2 tesla) below H_P of the sample with $n = 3$ for field along [100] and [001] directions of *STO* are shown in Fig. 4. The ZFC out-of-plane *MR* (Fig. 4b) is negative as well as positive with hysteretic and asymmetric nature. As the field sweep starts, the *MR* increases and shows a sharp change from positive to negative value at $+ H_{flip}$. On reverse sweep of H to zero from $+ 2$ tesla, the *MR* decreases with a lower value than the *MR* in the field-increasing branch. As H increases in the negative direction, the *MR* becomes positive until the field is smaller than $- H_{flip}$ and at $- H_{flip}$, the *MR* becomes negative. The negative field decreasing branch is similar but opposite to the reverse positive field sweep branch. In presence of H_{FC} the out-of-plane *MR* (Fig. 4a and 4c) is negative as well as positive, less hysteretic, more asymmetric and higher in magnitude compared to the ZFC *MR*. The ZFC in-plane *MR* (Fig. 4e) is negative, non-hysteretic and symmetric with respect to origin. In presence of H_{FC} , the (*MR - H*) curve becomes asymmetric (Fig. 4d and 4f). For a field applied along the direction of H_{FC} the in-plane *MR* is larger than the opposite direction field. Furthermore, the origin of the FC (*MR - H*) shows a small shift towards the field antiparallel to the H_{FC} . These phenomena are not the cumulative effect of the interfaces because of the shortening of the

top conducting layer. We attribute this asymmetric nature of the field-cooled ($MR-H$) loop to the *uniaxial pinning/biasing* of moments observed in the FC magnetic hysteresis loop.

The SRO/SMO superlattices exhibit anisotropy with the orientation of magnetic field to the sample in ($MR-H$) as well as ($M-H$) measurements. The major contributions to this anisotropy behavior is from the strong anisotropy of the SMO layers and the additional periodicity of the magnetic layer along the out-of-plane direction of the sample. The ZFC hysteresis loop measured with $H > H_P$ for both orientations of H indicates that the hard axis of SMO is along $[001]$ direction of STO (Fig. 1). At a field much below 4 *tesla* but larger than the H_S (0.4 *tesla*) of SRO , both H_C and magnetization (at 1 *tesla*) of the superlattice is lower compared to the thin film of SRO on STO by $\sim 95\%$ and $\sim 32\%$ in-the-film-plane and $\sim 84\%$ and $\sim 52\%$ out-of-plane respectively. This suggests that the ideal SRO/SMO magnetic structure (Fig. 5a) is lost as the sample is cooled down to 10 *K* due to the strong anisotropy of SMO layer, crystallographic and/or magnetic reconstructions and relaxation at the interfaces¹²⁻¹⁴. We attribute the suppression of H_C and magnetization to the pinning/biasing of SRO layer by the SMO layer due to the strong exchange coupling between them (at a field below H_P). At $H < H_P$ the magnetization results partially from the part of the SRO layer which rotates coherently with the magnetic field. This part of the SRO layer is identified as the free layer. Using this picture, we can model the ideal structure as a repetition of $AFM/(pin)/FM(Free)/(pin)$ unit (Fig. 5b). In the ZFC state, the net magnetization of the pin layer is negligible, i.e., antiferromagnetic orientation of the spin in the pin/bias layers. But in the FC state, the net magnetization of the pinned/biased layer is lower by the same value as $M_P^{\prime\prime}$ for in-plane H_{FC} , while for out-of-plane H_{FC} it is increasing to a finite value equal to M_P^{\perp} . Since M_P^{\perp} is much larger than the $\frac{M_R^+ - M_R^-}{2}$ on both ZFC and FC states, we conclude that the volume of the free layer is smaller than the volume of pinned/biased layer. Thus, the effective volume of the free layer depends on the SMO layer thickness, magnetic field and cooling field. Since the FC hysteresis loop of the superlattices shifts along the magnetization axis, this effect in SRO/SMO superlattices are seen at 0.1 *tesla* field low enough not to saturate the FM magnetization of SRO ($H_S =$

0.4 tesla), these processes must occur in the *SRO* layer. This is in contradiction with the shifts in FC hysteresis loop along the magnetic field axis, in a magnetic field high enough to saturate the *FM* magnetization - where the irreversible process occurs at the interfaces and in the *AFM*¹⁻⁵. In the range of 1 tesla ($< H_P$) magnetic field, the orientation of spin in *SMO* layer is along the film-plane, for field along [100] and [001] directions of *STO*. Since the anisotropy axis of *SMO* layer is fixed, the magnetic field along the easy axis of *SMO* layer, decreases the angle between the magnetization of *SRO* layer and the easy axis of *SMO* layer, while their angular separation increases as the magnetic field is rotated 90°. So, the in-plane H_{FC} may induce bilinear coupling of the spins of *SMO* and *SRO* at the interfaces, while the out-of-plane H_{FC} induces biquadratic coupling.

Transport processes in magnetic structures as spin-dependent tunneling¹⁵ and scattering of spin-polarized carriers¹⁶ are influenced by the spin-orientations of the pinned/biased layers and free layers of *SRO*. The *FC* magnetic field dependent *MR* in this structure can be explained by using the spin dependent scattering¹⁷ and the uniaxially pin/bias spin. When the net moment in the pin and free layers are parallel, the in-plane *MR* is higher and out-of-plane *MR* is negative; while the antiparallel alignment of the net moments in the bias/pin and free layers results in a lower in-plane *MR* and a positive out-of-plane *MR*. This correlation between the *FC* out-of-plane magnetization and *MR* with the change in magnetic field is sketched in Fig. 5(c).

In summary, the magneto-transport properties of *SRO/SMO* superlattices deposited on (001) – *STO* substrates were studied. Our data provide the direct evidence for the *manifestation of the uniaxial pinned/biased moments* in the *FM/AFM* superlattice. The pinned/biased moments becomes uniaxial as the superlattice is cooled in presence magnetic field. The in-plane cooling field orients pinned/biased moments antiferromagnetically while they orient ferromagnetically with the out-of-plane cooling field. The electronic transport in these superlattices shows the evidence of spin coupling of the mobile carriers to the interfacial pinned/biased layer. The field dependent in-plane *MR* is negative while the out-of-plane *MR* is negative as well as positive. We explain the magnetization and *MR* by

the spin dependent scattering due to the relative orientation of the net magnetization of the pinned/biased and free layers. Since progress towards understanding and use of spin-electronic is growing rapidly, these results should provide fundamentally new advances in both pure and applied sciences.

Acknowledgments:

We thank A. Fert, J.M. Triscone, B. Raveau, B. Mercey, A. Pautrat, A. Maignan and H. Eng for their helpful discussions. This work is supported by the Centre Franco-Indien pour la Promotion de la Recherche Avancee/Indo-French Centre for the Promotion of Advance Research (CEFIPRA/IFCPAR) under Project N°2808-1.

REFERENCES

- ¹ W.H. Meiklejohn and C.P. Bean, *Phys. Rev.* **102**, 1413 (1956).
- ² J. Nogués, and I.K. Schuller, *J. Magn. Magn. Mater.* **192**, 203 (1999).
- ³ A. E. Berkowitz and K. Takano, *J. Magn. Magn. Mater.* **200**, 552 (1999).
- ⁴ R. L. Stamps, *J. Phys. D* **33**, R247 (2000).
- ⁵ M. Kiwi, *J. Magn. Magn. Mater.* **234**, 584 (2001).
- ⁶ H. Ohldag, A. Scholl, F. Nolting, E. Arenholz, S. Maat, A.T. Young, M. Carey, and J. Stöhr, *Phys. Rev. Lett.* **91**, 017203 (2003).
- ⁷ S. Maat, K. Takano, S.S.P. Parkin, and E.E. Fullerton, *Phys. Rev. Lett.* **87**, 087202 (2001).
- ⁸ P. Padhan, W. Prellier, and B. Mercey *Phys. Rev. B* **70**, 184419 (2004).
- ⁹ G. Cao, S. McCall, M. Shepard, J. E. Crow, and R. P. Guertin, *Phys. Rev. B* **56**, 321 (1997).
- ¹⁰ L. Klein, J. S. Dodge, T. H. Geballe, A. Kapitulnik, A. F. Marshall, L. Antognazza and K. Char, *Appl. Phys. Lett.* **66**, 2427 (1995).
- ¹¹ T. Takeda and S. Ohara, *J. Phys. Soc. Jpn.* **37**, 275 (1974).
- ¹² P. Padhan, R.C. Budhani and R.P.S.M. Lobo, *Europhys. Lett.* **63**, 771 (2003).
- ¹³ P. Padhan, and R.C. Budhani, *Phys. Rev. B* **67**, 024414 (2003).
- ¹⁴ M. Izumi, T. Manako, Y. Konishi, M. Kawasaki and Y. Tokura, *Phys. Rev. B* **61**, 12187 (2000).
- ¹⁵ G. Herranz, B. Martínez, J. Fontcuberta, F. Sánchez, M.V. García-Cuenca, C. Ferrater, and M. Varela, *J. Appl. Phys.* **93**, 8035 (2003).
- ¹⁶ B. Nadgorny, M.S. Osofsky, D.J. Singh, G.T. Woods, R. J. Soulen, Jr. , M.K. Lee, S.D.

Bu, and C.B. Eom, *Appl. Phys. Lett.* **82**, 427 (2003).

¹⁷ M.N. Baibich, J.M. Broto, A. Fert, F.N.V. Dau, F. Petroff, P. Etienne, G. Creuzet, A. Friederich, and J. Chazelas, *Phys. Rev. Lett.* **61**, 2472 (1988).

Figures Captions:

Fig. 1: Isothermal (10 K) zero-field-cooled magnetization of the (20 u.c.) *SRO*/(3 u.c.) *SMO* superlattice at various fields oriented along the [100] and [001] directions of the substrate, respectively.

Fig.2(a) and (b): Isothermal (10 K) zero-field-cooled and field-cooled magnetization of the (20 u.c.) *SRO*/(3 u.c.) *SMO* superlattice at various fields oriented along the [100] and [001] directions of the substrate, respectively.

Fig. 3 Out-of-plane field-cooled biased/pinned moment (M_P^\perp) of several superlattices at 10 K.

Fig.4 Current-in-plane zero-field-cooled and field-cooled magnetoresistance MR ($MR = \frac{R(H)-R(H=0)}{R(H)}$) of the (20 u.c.) *SRO*/(3 u.c.) *SMO* superlattice at various fields at 10 K. Panels a, b and c show the -0.1 tesla *FC*, *ZFC*, and 0.1 tesla *FC* magnetoresistance respectively at various magnetic fields along the [001] direction of the substrate. Panels d, e and f show the -0.1 tesla *FC*, *ZFC*, and 0.1 tesla *FC* magnetoresistance respectively at various magnetic fields along the [100] direction of the substrate. The arrows indicate the directions of the field sweep with the thicker arrow denoting the commencement.

Fig. 5(a) and (b) Schematic view of the cross section of two interfaces of *SRO*/*SMO* multilayer at room temperature and 10 K, respectively. (c) Schematic comparison of *FC* magnetization and magnetoresistance measured with magnetic field lower than the critical pinning field oriented along the [001] direction of the substrate. In the rectangle box, thick and thin arrows represent the relative orientations of the pinned and free layer net moments, respectively.

Fig. 1 Padhan and Prellier

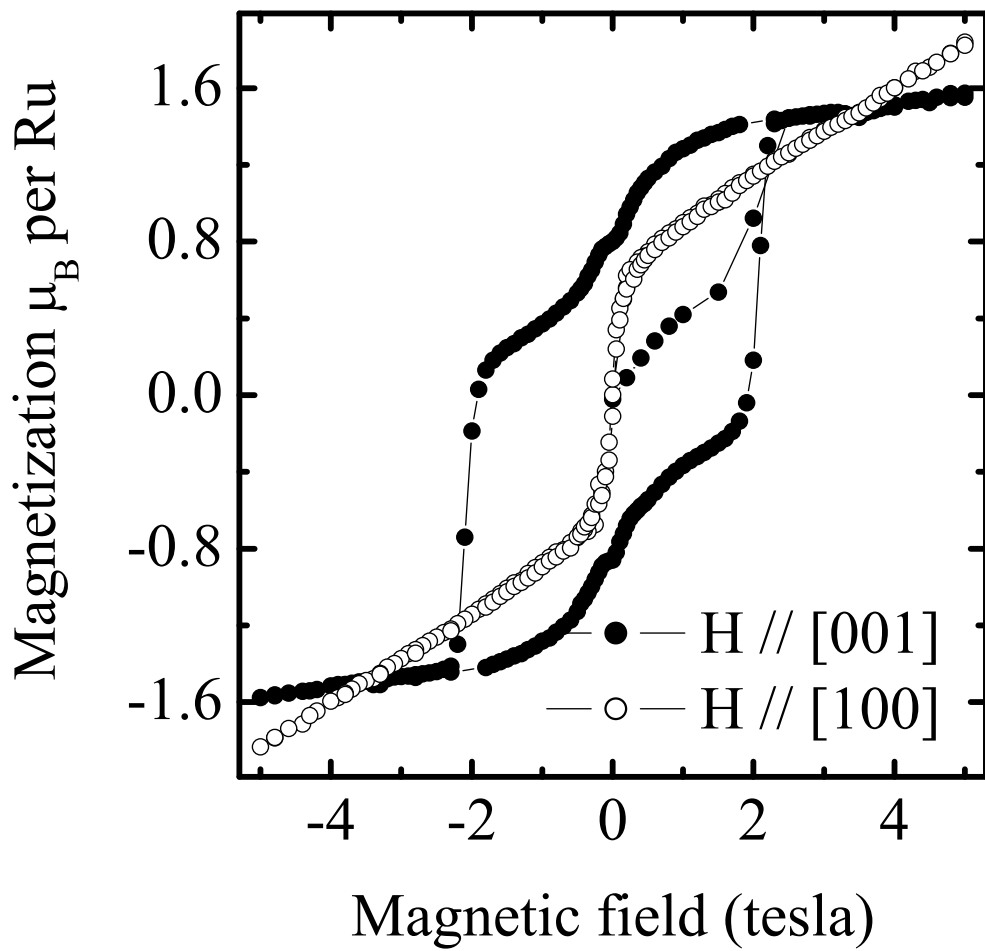


Fig. 2 Padhan and Prellier

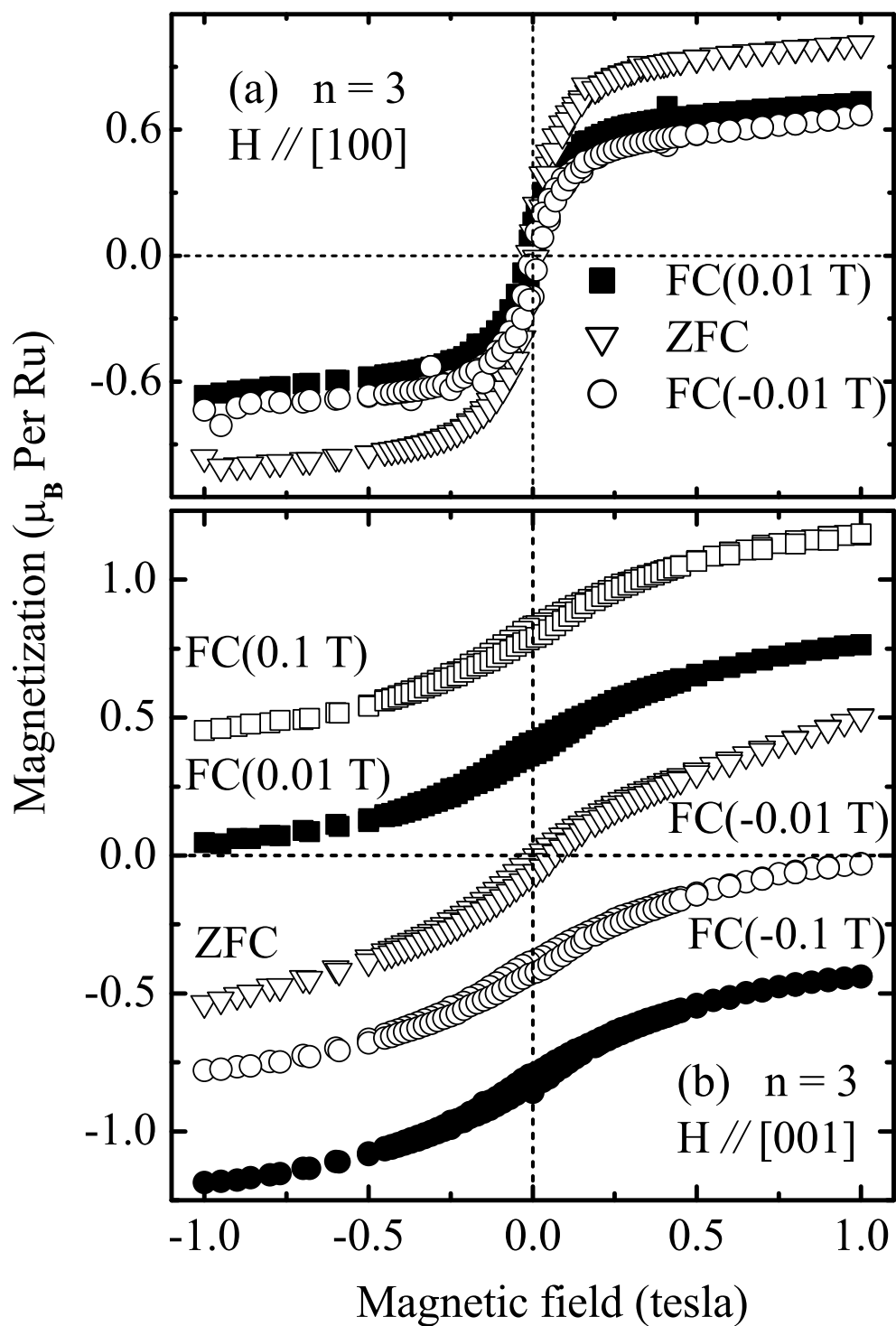


Fig. 3 Padhan and Prellier

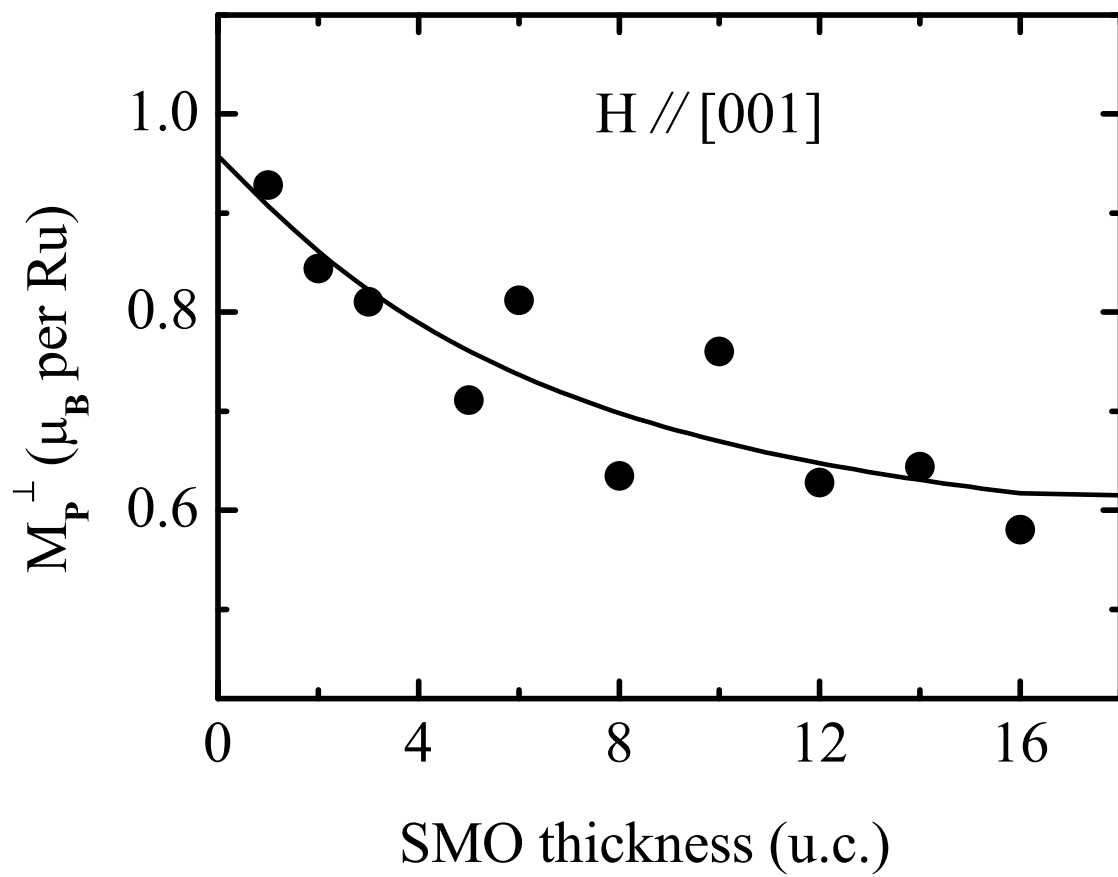


Fig. 4 Padhan and Prellier

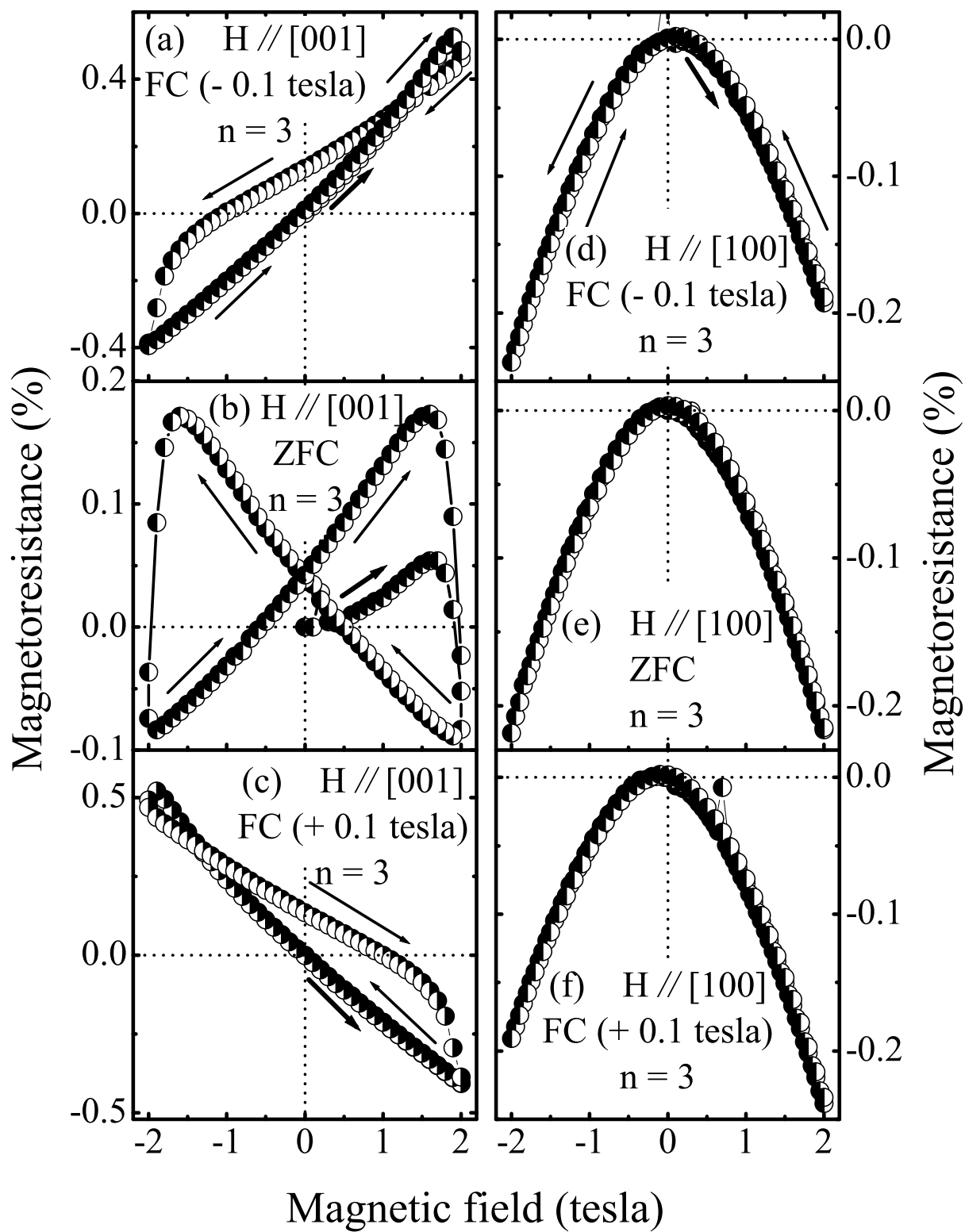


Fig. 5 Padhan and Prellier

